1 Title:

2 Health and disease imprinted in the time variability

3 of the human microbiome

4 Running title:

5 Microbiota, are you sick?

6 **Jose Manuel Martí**[1,2,*], **Daniel Martínez-Martínez**[1,2,3,*], **Manuel Peña**[2], **César Gracia**[1,2],

7 **Amparo Latorre**[1,3,4,5], **Andrés Moya**[1,3,4,5] **& Carlos P. Garay**[1,2,#]

8 [1]Institute for Integrative Systems Biology (I2SysBio), 46980, Spain.

9 [2]Instituto de Fisica Corpuscular, CSIC-UVEG, P.O. 22085, 46071, Valencia, Spain.

10 [3]FISABIO, Avda de Catalunya, 21, 46020, Valencia, Spain.

11 [4]Cavanilles Institute of Biodiversity and Evolutionary Biology, UVEG, 46980, Spain.

12 [5]CIBER en Epidemiología y Salud Pública (CIBEResp), Madrid, Spain

13 Words count for the Abstract section: 154 of 250 max

14 Words count for the Importance section: 105 of 150 max

15 Words count for the rest of text: 4890 of 5000 max

16

[*] Equally contributed

[#] Corresponding author: penagaray@gmail.com

Abstract

Animal microbiota (human included) plays an important role keeping healthy the physiological status of the host. Increasing research activity is dedicated to understand how changes in composition and function of the microbiota are associated to disease or not. We analyze 16S rRNA and whole genome sequencing (WGS) published data from the gut microbiota of 97 individuals monitored in time. Temporal fluctuations in the microbial composition reveal significant differences due to factors such us dietary changes, antibiotic intake, age or disease. Here we show that a fluctuation scaling law describes the temporal changes in the gut microbiota. This law allows to estimate the temporal variability of the microbial population and quantitatively characterizes the path toward disease by a noise-induced phase transition. The estimation of the systemic parameters for follow-up studies may have clinical use and, more generally, applications in other fields where it is important to know if a given community is stable or not.

Importance

Human microbiota is tightly associated to the health status of a person. Here we analyse the microbial composition of several subjects under different conditions, over a time span that ranges from days to months. Using the Langevin equation as the basis of our mathematical framework in order to evaluate microbial temporal stability, we prove that we are capable to distinguish stable from unstable microbiotas. This first step will help us to determine how microbiota temporal stability is related to the healthiness of the people, and it will allow the development of a more complete framework in order to deepen the knowledge of this complex system.

Introduction

The desire to understand the factors that influence human health and cause diseases has always been one of the major driving forces of biological research. As evidence of new concepts 'holobiont' and 'hologenome' is increasing each day (*1, 2*), research not only focus on the human physiology but also on the microbial population that surround ourselves. We are populated by a myriad of microorganisms that are interacting with us in several physiological processes such as metabolism of the bile acids (*3*), of the choline (*4*) or key-route metabolites as short-chain fatty acids (*5, 6*) which are also involved in immune system maturation (*7, 8*). Human microbiota has been suggested to be closely related to diseases like type 2 diabetes (*9*), cardiovascular disease (CVD) (*10*), irritable bowel syndrome (*11*), Crohn's disease (*12*), some affections as obesity (*13, 14*), malnutrition (*15*) among other multiple diseases (*16*). High throughput methods for microbial 16S ribosomal RNA gene and WGS have now begun to reveal the composition of archaeal, bacterial, fungal and viral communities located both, in and on the human body. Modern high-throughput sequencing and bioinformatics tools provide a powerful means of understanding how the human microbiome contributes to health and its potential as a target for therapeutic interventions (*17*). To define normal microbiota and how it's compositional changes can origin some diseases are important issues still in need for scientific answers (*18, 19*).

Biology has recently acquired new technological and conceptual tools to investigate, model and understand living organisms at the system level, thanks to the spectacular progress in quantitative techniques, large-scale measurement methods and the integration of experimental and computational approaches. In particular, Systems Biology has placed a great effort to unveil the general laws governing the complex behaviour of microbial communities (*20–22*). Microbiota can be approached under the light of ecological theory where we can find, for instance, general principles as the Taylor's law (*23*), which relates spatial or temporal variability of the population with its mean. This law, also known as fluctuation scale law, is

65 ubiquitous in the natural world and can be found in several systems as random walks (*24*),

66 stock markets (*25, 26*), animal populations (*23, 27, 28*), gene expression (*29*), or in the hu-

67 man genome (*30*). Taylor's law has been applied to microbiota in a spatial way in the work of

68 Zhang *et al.*, (2014) (*31*), where they show that this population tend to be in an aggregated

69 way rather than in a random distribution. Despite its ubiquity, it has been studied only in

70 experimental settings (*32, 33*) but never been applied in follow-up studies from microbiota

71 even that a great effort has been made to infer the community structure from a dynamical

72 point of view (*34–36*)

73 Here we present the imprints of health status (healthy or disease) in macroscopic properties

74 of microbiota, by studying its temporal variability. We have analyzed more than 35000 time

75 series of taxa from the gut microbiome of 97 individuals obtained from publicly available high

76 throughput sequencing data on different conditions: diseases, diets, obese status, antibiotic

77 therapy and healthy individuals. Having seen that all cases follows Taylor's law, we use this

78 empirical fact to model how the relative abundances of taxa evolves toward time thanks to the

79 Langevin equation, in a similar way as it was applied recently by Blumm *et al.* (*37*). We use

80 this mathematical framework to explore the temporal stability of the microbiota in different

81 conditions in order to understand how this affects the healthy status of the subjects.

Results

We have analysed the microbiome temporal variability to extract global properties of the system. As fluctuations in total counts are plagued by systematic errors we worked on temporal variability of relative abundances for each taxon. Our first finding was that, in all cases, changes in relative abundances of taxa follow a ubiquitous pattern known as the fluctuation scaling law (*46*) or Taylor's power law (*23*), i.e., microbiota of all detected taxa follows $\sigma_i = V \cdot x_i^\beta$, a power law dependence between mean relative abundance x_i and dispersion σ_i. The law seem to be ubiquitous, spanning even to six orders of magnitude in the observed relative abundances (see Figure 1).

The power law (or scaling) index β and the variability V (hereafter Taylor parameters) appear to be correlated with the stability of the community and related with the health status of the host, which we consider the main finding exposed in this article (see Figure 2).

Taylor parameters describing the temporal variability of the gut microbiome in our sampled individuals are shown in Tables S1 to S6. Our results hint at an ubiquitous behaviour. On the first hand, the variability (which corresponds to the maximum amplitude of fluctuations) is large, which suggests resilient capacity of the microbiota. On the other hand, the scaling index is always smaller than one, which means that more abundant taxa are less volatile than less abundant ones. In addition, Taylor parameters for the microbiome of healthy individuals in different studies are compatible within estimated errors. This enables us to define an area in the Taylor parameter space that we called the *healthy zone*.

In order to jointly visualize and compare the results of individuals from different studies, their Taylor parameters have been standardized, where standardization means that each parameter is subtracted by the mean value and divided by the standard deviation of the group of healthy individuals for each study (for details of the procedure, please see Standardization subsection in Material and Methods). The healthy zone and the standardized Taylor parame-
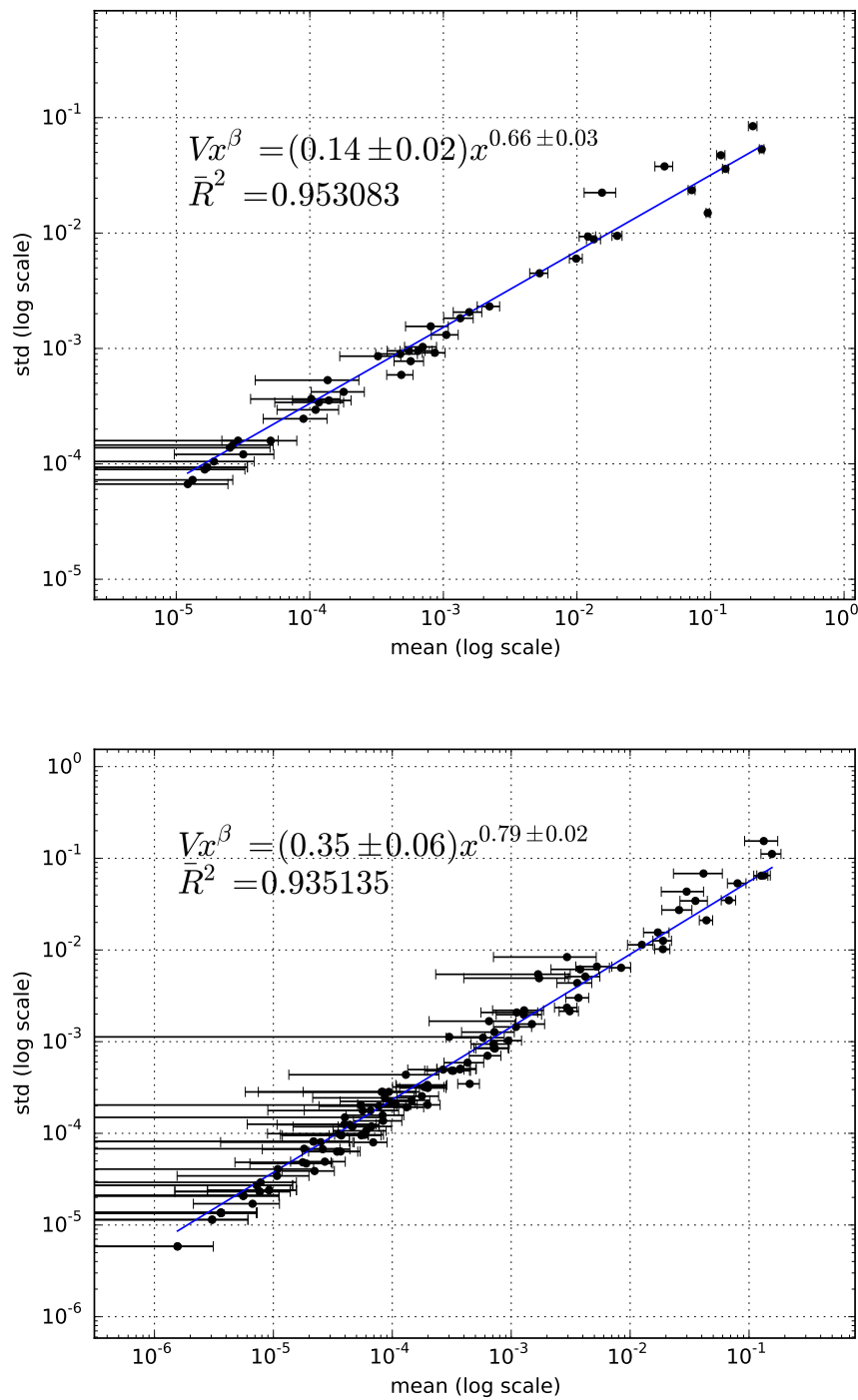
$$Vx^{\beta} = (0.14 \pm 0.02)x^{0.66 \pm 0.03}$$
$$\bar{R}^2 = 0.953083$$

$$Vx^{\beta} = (0.35 \pm 0.06)x^{0.79 \pm 0.02}$$
$$\bar{R}^2 = 0.935135$$

Figure 1. X-weighted power-law fits of the standard deviations versus the mean values for each bacterial genus monitored in time. We show the fit for samples from a healthy subject (top) and from a subject diagnosed with irritable bowel syndrome (bottom), studied in our lab (*11*). Taylor's power law seems to be ubiquitous, spanning to six orders of magnitude.
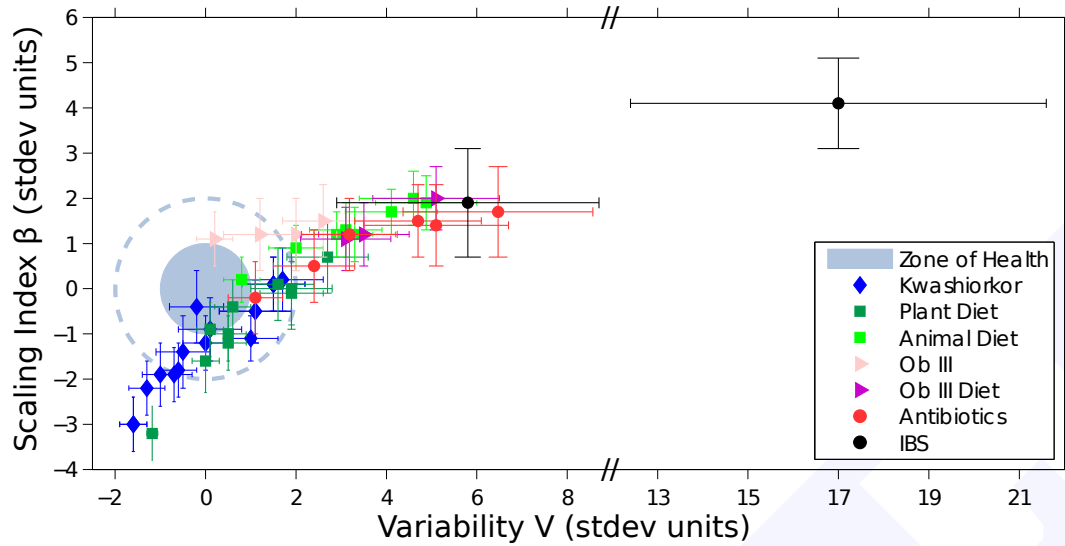
Figure 2. Taylor's law parameter space. We have compiled here all the data studied in this work. The coloured circle corresponds to 68% confidence level (CL) region of healthy individuals in the Taylor parameter space, while dashed line delimites the 98% CL region. Points with errors place each individual gut microbiome in the Taylor space. Note that the parameters have been standardized (stdev units) to the healthy group in each study for demonstrative and comparative purposes.

107 ters for individuals whose gut microbiota is altered (i.e., suffering from kwashiorkor, altered

108 diet, antibiotics or IBS) is shown in Figure 2. Children developing kwashiorkor show smaller

109 variability than their healthy twins. A meat/fish-based diet increases the variability signifi-

110 cantly when compared to a plant-based diet. All other cases presented increased variability,

111 which is particularly severe, and statistically significant at more than 95% CL, for obese pa-

112 tients grade III on a diet, individuals taking antibiotics or IBS–diagnosed patients. A global

113 property emerges from all worldwide data collected: Taylor parameters characterize the sta-

114 tistical behavior of microbiome changes. Furthermore, we have verified that our conclusions

115 are robust to systematic errors due to taxonomic assignment (see Figure Sx in Supplemental

116 Material).

117 Taylor's power law has been explained in terms of various effects, all without general consen-

118 sus. It can be shown to have its origin in a mathematical convergence similar to the central

119 limit theorem, so virtually any statistical model designed to produce a Taylor law converge

120 to a Tweedie distribution (*47*), providing a mechanistic explanation based on the statistical

121 theory of errors (*48–50*). To unveil the generic mechanisms that drive different scenarios in

122 the β–V space, we model the system by assuming that taxon relative abundance follows a

123 Langevin equation with, on the one hand, a deterministic term that captures the fitness of

124 each taxon and, on the other hand, a randomness term associated with Gaussian random

125 noise (*37*). Both terms are modeled by power laws, with coefficients that can be interpreted

126 as the taxon fitness F_i and the variability V (see Model under Material and Methods). In this

127 model, when V is sufficiently low, abundances are stable in time. Differences in variability

128 V can induce a noise-induced phase transition in relative abundances of taxa. The temporal

129 evolution of the probability of a taxon having abundance x_i given its fitness is governed by

130 the Fokker–Planck equation. The results of solving this equation show that the stability is

131 best captured by a phase space determined by fitness F and amplitude of fluctuations V (see
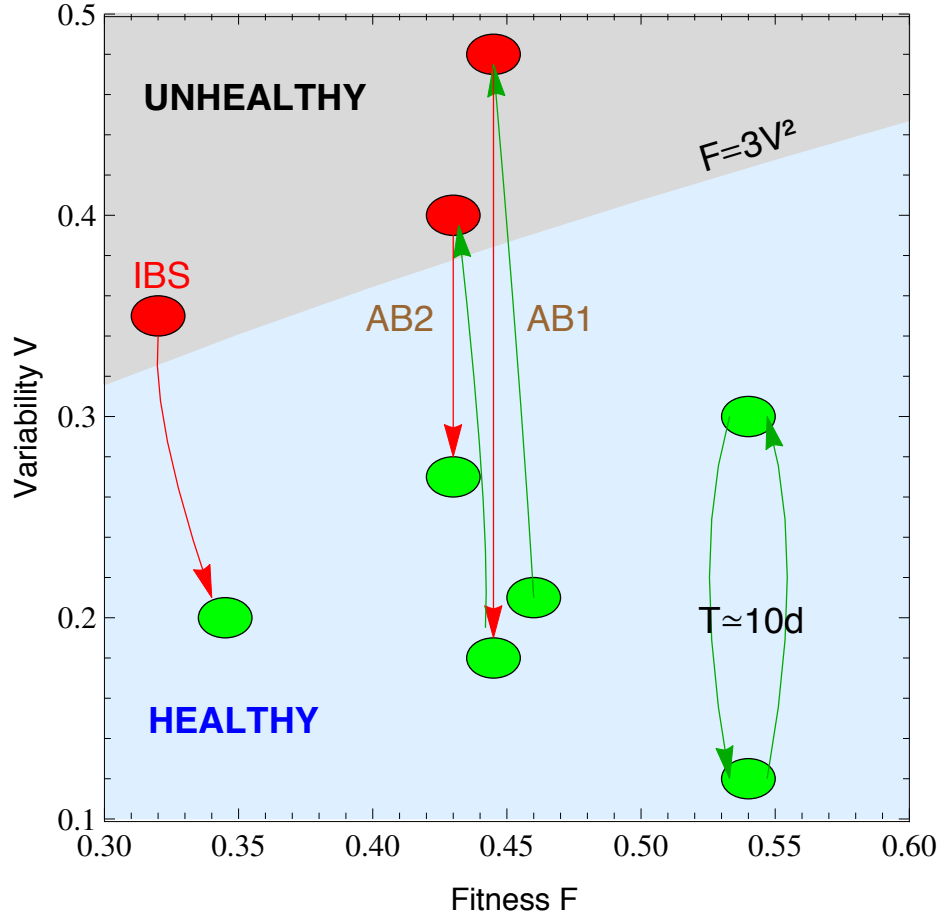
132 Figure 3).

Figure 3. Microbiota states can be placed in the phase space F–V. The light blue shaded region corresponds to the stable phase, while the grey shaded region is the unstable phase (the phase transition line is calculated for $\alpha = \beta = 0.75$). We place healthy individuals (green) and individuals whose gut microbiota is threatened (antibiotics, IBS) in the phase space fitness–variability. Gut microbiota of healthy individuals over a long term span show a quasi–periodical variability (central period is ten days). We show that taking antibiotics (AB1 and AB2 correspond to first and second treatment respectively) induces a phase transition in the gut microbiota, which impacts its future changes. We also show an IBS–diagnosed patient transiting from the unstable to the stable phase.

133 The model predicts two phases for the gut microbiome: a stable phase with large variability

134 that permits some changes in the relative abundances of taxa and an unstable phase with

135 larger variability, above the phase transition, where the order of abundant taxa varies signif-

136 icantly with time. The microbiome of all healthy individuals was found to be in the stable

137 phase, while the microbiome of several other individuals was shown to be in the unstable

138 phase. In particular, individuals taking antibiotics and IBS–diagnosed patient P2 had the

139 most severe symptoms. In this phase diagram, each microbiota state is represented by a

140 point at its measured variability V and inferred fitness F. The model predicts high average

141 fitness for all taxa, i.e., taxa are narrowly distributed in F. The fitness parameter has been

142 chosen with different values for demonstrative purposes. Fitness is larger for the healthiest

143 subjects and smaller for the IBS–diagnosed patients.

Rank stability of the taxa

145 The rank dynamics and stability plot in Figure 4 shows the variation in the rank with time

146 for the most dominant taxa and their calculated Rank Stability Index (RSI, as discussed in

147 Material and Methods) for the taxa of a healthy subject (individual A, top) and from a subject

148 diagnosed with IBS (patient $P2$, bottom) of the IBS study (*11*). The taxa are listed ordered

149 by the accumulated frequency along the time series, so y-axis is an overall dominance axis for

150 each sample set. Generally speaking, we observe that the most dominant taxa are the most

151 rank stable.

152 Nevertheless, in the particular case of the healthy individual, *Burkholderiales* and *Betapro-*

153 *teobacteria* (taxa ordered as 18th and 25th in the dominance axis) show comparatively very

154 low rank stability regarding similar dominant taxa while, on the other hand, *Comamon-*

155 *adaceae, Lactobacillaceae, Fusobacteriaceae, Aerococcaceae* and *Carnobacteriaceae* show higher

156 stability than other more dominant taxa, forming a kind of *rank stability island* for medium-
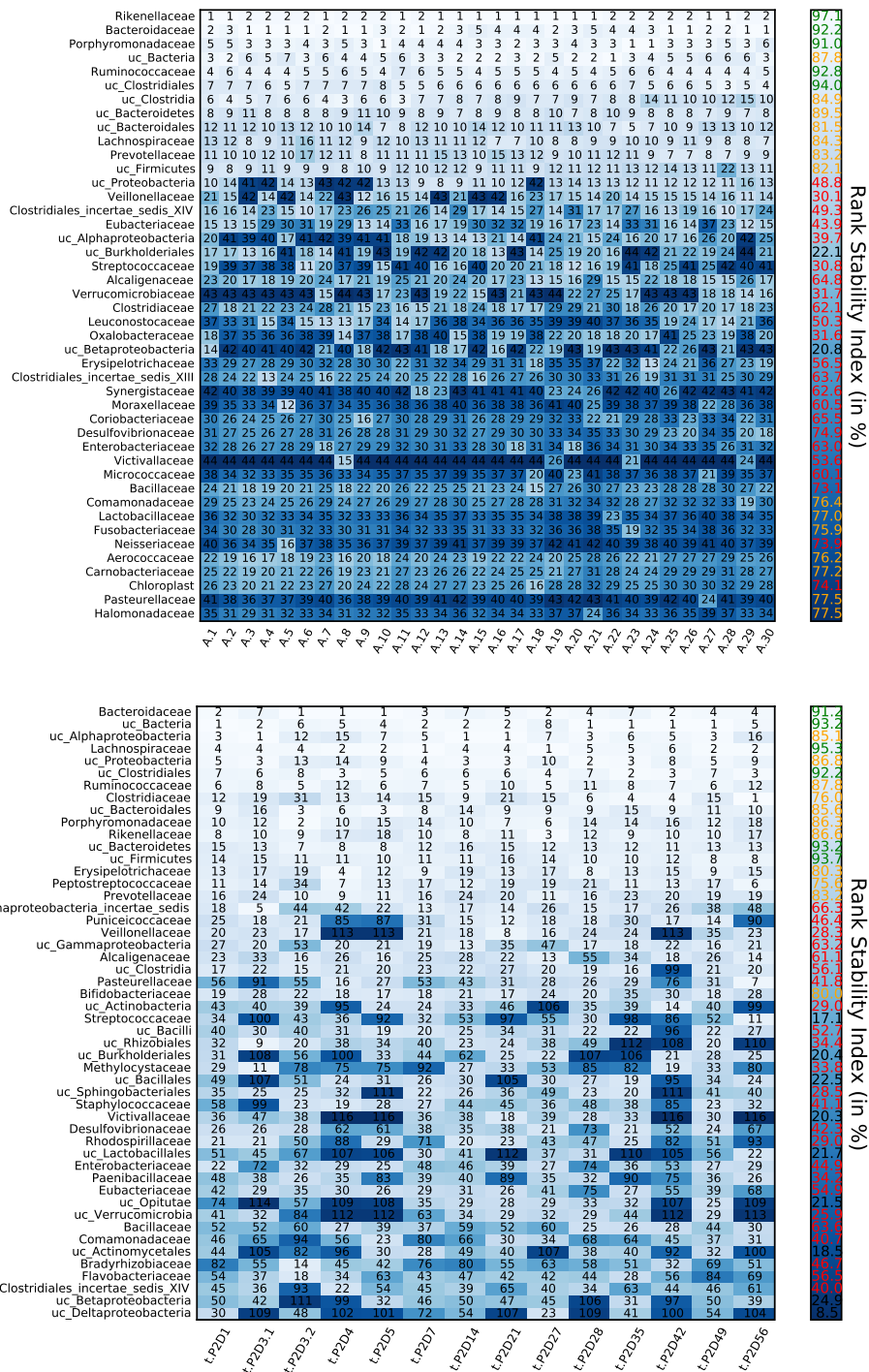
10

Figure 4. Matrixes showing the rank variation throughout time for the most dominant elements (taxa) and their calculated Rank Stability Index (as discussed in Material and Methods). We show the matrix for samples from a healthy subject (top) and from a subject diagnosed with irritable bowel syndrome (bottom), studied in our lab (*11*).

ranked taxa around position 40 in the dominance axis, and thus colored in orange following Table 1 criteria, since they show a moderately stable RSI.

In the IBS diagnosed patient, beyond the differences in dominance for the particular taxa, we still observe that the most dominant are the most rank stable. However, as opposed to the healthy individual results, far from presenting a *rank stability island*, the medium-ranked taxa are very rank unstable, mostly due to transient (often one or two consecutive samples) but deep drops in their relative abundance, which are usually happening more than twice along the time series. That is, for instance, the case of *Sphingobacteriales* with two non-consecutive samples dropping to 111th rank position. In other cases, the high rank instability comes from a rank fluctuation over all the time series, as for *Streptococcaceae* and *Burkholderiales*, which are ranking 26th and 29th respectively in the overall dominance axis but show very low RSI, and thus colored in black attending to Table 1.

We found the presence of such of *rank stability island* for medium-ranked taxa in the other healthy subjects (*B* and *C*) of the IBS study (*11*) together with its total absence for the other IBS diagnosed patient (patient *P1*), which also presents very high rank instability in its medium-ranked taxa.

Time dependence of model parameters

Finally, we have studied the time dependence of the variability V and power law index β (see Model under Material and Methods) by using a sliding window approach. The total number of time points are divided in subsets of five points, where next subset is defined by adding next time sampling and by eliminating the earliest one. Both parameters were calculated for each subset against the average time lapse. Figure 5 shows the variability V as a function of time for the largest sampling: two individuals in the Caporaso's study (*38*) corresponding to the gut microbiota of a male (upper plot) and a female (lower plot). Figure 6 shows the
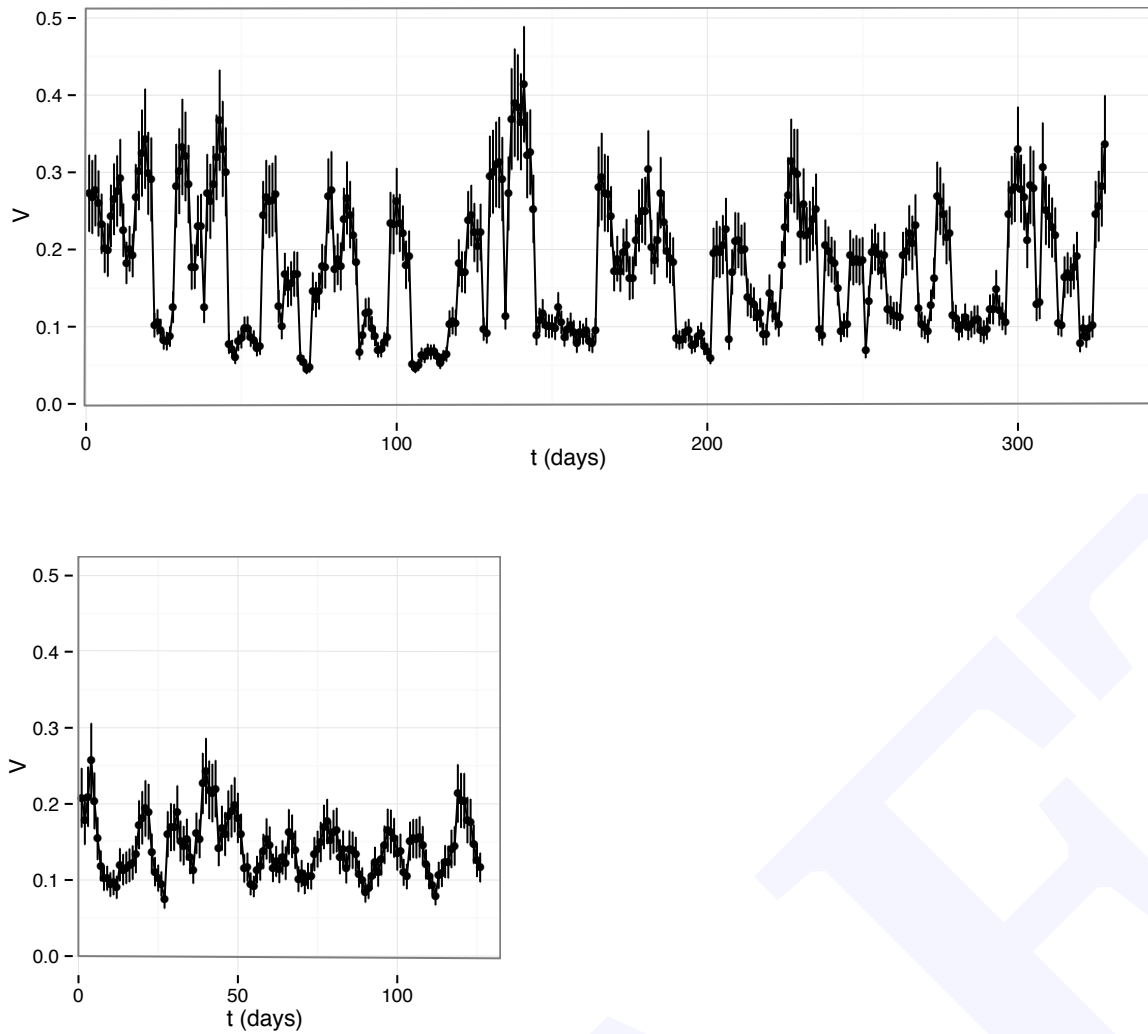
Figure 5. *V* as a function of time for the two individuals in the Caporaso's study (*38*): samples of gut microbiome of a male (upper plot) and a female (lower plot). Both samples show changes in the variability V with quasi–periodic behavior peaked at about 10 days. Variability grows more for the gut microbiota of the male and share a minimal value around 0.1 with the gut microbiota of the female.

181 time evolution of *V* for patient P2 of the IBS study (*11*) (upper plot) and patient D in the
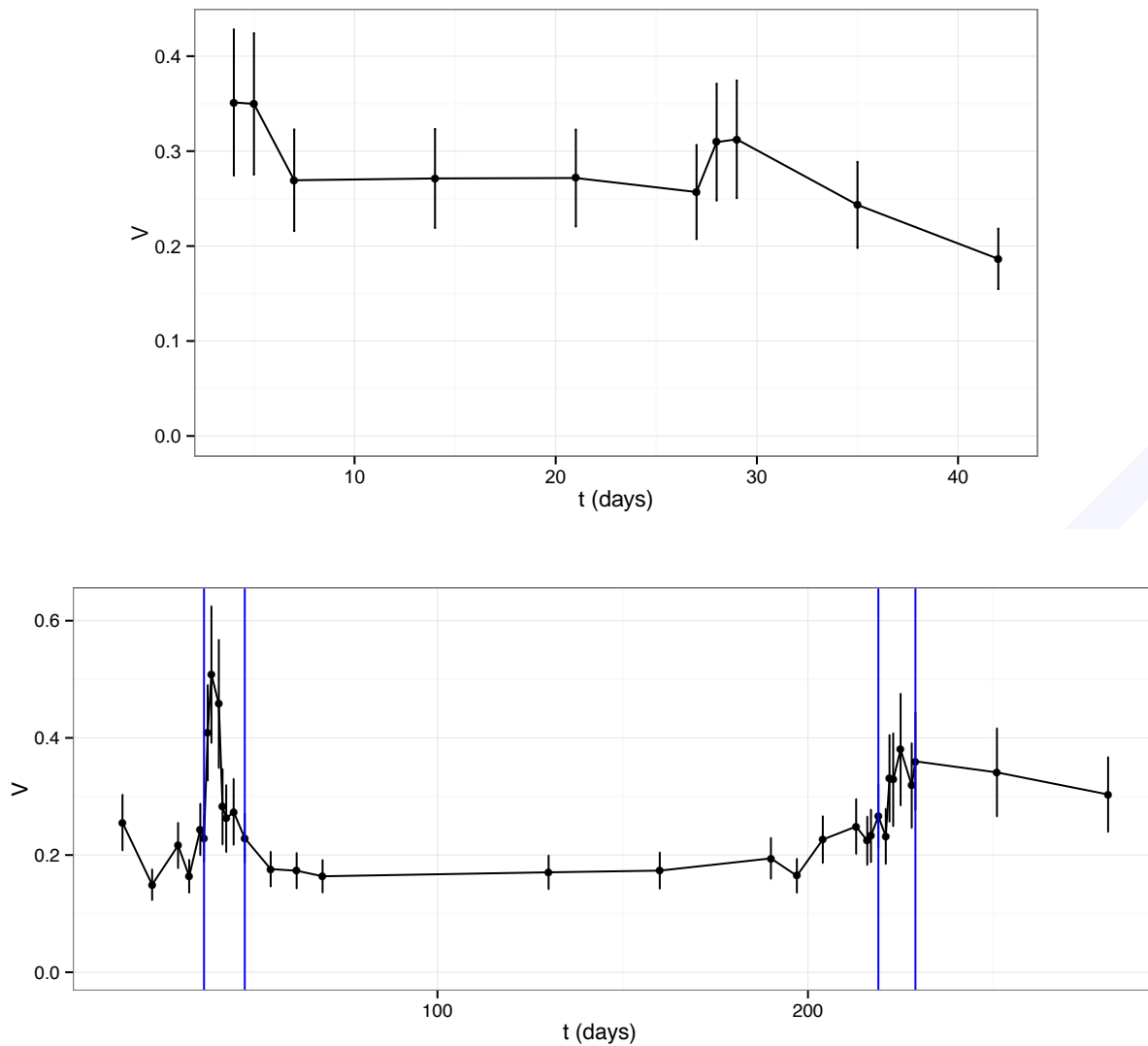
182 antibiotics study (*42*) (lower plot).

Figure 6. *V* as a function of time for patient P2 of the IBS study (*11*) (upper plot) and patient D in the antibiotics study (*42*) (lower plot). The variability of the gut microbiota of P2 decreases from above 0.3 to below 0.2, showing a slow tendency to increase the order of the system. Antibiotic intake leaks to a quick increase of variability which lasts for a few days to recover ordering. The second antibiotic treatment shows some memory (lower increase of variability) with a slower recovery. NOTE: The blue vertical lines in the lower plot are showing the periods of antibiotic treatment.

Discussion

One of the mains features of this work is to have shown that the microbiota, independently of its condition, follows the Taylor's law. We have seen that the value of the scaling index in each case is always less than the unity (using standard deviation in the law), which is informing us about the community structure. This means that the most abundant elements in the population are less volatile to perturbations in relative terms than the less abundant. The explanation for this universal pattern is not clear although some hypothesis have been tested in other studies as the presence of negative interactions in the population (*51*), while others have demonstrated that it may depend on reproductive correlation (*52*). Nevertheless, none of these explanations are enough when we are talking about microbiota as the reproduction term is diffuse, the interactions between its components are not only based on competition (*53–55*) and that kind of negative interaction may not effectively yield in values less than the unity when referring to a bacterial species (*33*). In any case, the values obtained in all cases are very similar between them, hence these theoretical questions may be addressed in future works.

The second parameter is informing about the noise and can be directly related with the variability or the fluctuation amplitude of the population over time, and it is a direct estimator of the stability of the system under study. As we showed in above, the healthy part of each study have lower variability than the non-healthy part when dealing with adult individuals. Interestingly, the variability parameter was higher in the healthy part of the study of the discordant twins suffering from kwashiorkor disease (*40*). Taking into account that the infant microbiota is evolving toward a definite, adult state (*57*), it means that the temporal variability would be greater than in a adult who has reached a stability in his gut microbiota, while our results could be directing in the possibility that this variability is necessary in order to reach that adult state. Furthermore, as we wanted to see how this variability was over time, we calculated the evolution of this parameter for the samples which had enough time sam-

15

209 pling. As can be seen in Figure 5, the variability of the microbiota has some fluctuations over

210 time. It is interesting to note in Figure 6 how this parameter can capture the two antibiotic

211 intakes in one of the patients from the study of Dethlefsen and Relman (*42*), especially that

212 it seems to be some resiliance process in the microbiota due to the lower variability increase

213 in the second antibiotic intake.

214 The primary hypothesis of this work is that having a healthy microbiota means, in adult

215 individuals, that population is stable in time and does not have huge flips or jumps into

216 another states. In order to use the valuable information which gives us the empirical law of

217 Taylor's work, we propose the use of Langevin equation to model how the ranking stability

218 evolves in time. While we can measure directly the component of the noise of the system as

219 their variability, the other main term needs to be inferred from the model. This term, which we

220 have named as 'fitness', is the one that gives the ability to the system to be stable to a possible

221 perturbations. In ecological terms, this could mean the nature of interactions that are present

222 between the bacteria, between bacteria and other minority populations as fungi or archaea,

223 between bacteria and the viral component in the microbiota, and the interactions between

224 host and the whole microbiota. Being this a first step to model the temporal stability of the

225 microbiota and due to its complicated nature, we have calculated the fitness term using the

226 fluctuation-dissipation theorem as a first approximation. Thus, the fitness of the microbiota

227 still remains to be modeled in future works in order to make the model more accurate and

228 with a higher predictive power.

229 By solving the Langevin differential equation, we can obtain a phase diagram where each

230 microbiota sample can be placed according to its fitness and variability in one of the two

231 phases according to the ranking stability of the system. As we can see in the phase space in

232 Figure 3, we are showing three different conditions that could happen. First, we can have a

233 healthy microbiota which could have some fluctuations as showed by one of the subjects of

234 Caporasso et al study (*38*). Because the fitness of this cases will be high enough, the temporal

16

variability will not place the microbiota in the unstable phase of the diagram. Second, we have a subject from the study of Dethlefsen and Relman (*42*) which is perturbed twice by an antibiotic intake. His microbiota is altered enough to loose its stability and then be placed in the unstable part, being more sensible to a possible perturbations as, for example, opportunist infections. Third, the subject is already in the unstable phase due to some healthy issue as IBS, as can be observed in one of the patients from Durban et al study (*11*). It is shown also that this subject improved its healthy status in the time when the experiment was done, implying that his microbiota also recovered the lost stability.

Specifically, the analysis of the rank stability of the samples of healthy and IBS diagnosed patients studied in our lab (*11*), suggests that the presence of a *rank stability island* among medium-ranked taxa could be an indicator of a healthy microbiota. (to complete)

But we have to be aware that the hypothesis above is too simplistic to be related with the reality. It has been demonstrated that the situation is more complex than to separate healthy people from non-healthy people by compositional terms only as Moya and Ferrer underlines in their review (*16*). There are several different scenarios that can be possible in which we can consider the microbiota as stable independently of their compositional evolution over time, as for example in their ability to recover the initial composition (resiliance), or if it can recover the original function despite the composition (functional redundancy). What we have showed in this work could be explained as the transitions of a stable microbiota into a dysbiosis state.

As a first step toward understanding the microbiota stability, the model present some limitations and there is still work to do. From the biological perspective, many questions arise from this work as for example which mechanisms are involved in maintaining the population structure. The nature of the interactions between the elements of the community is surely of great importance in this matter, and it is related to the fitness of the community as has been commented above. To capture these interactions, we could try to use the generalized Lotka-

261 Volterra system of differential equations or other methods which are mathematically similar.

262 There are also other ways in which we could infer the community fitness without taking into

263 account the interactions as has been exposed by Tikhonov (*58*). There is also the possibility

264 to work with the fluctuation-dissipation theorem and try to understand what could mean the

265 'temperature' in ecological terms.

Materials and Methods

Model

We model the microbial abundances across time along the lines of Blumm *et al.* (*37*). The dynamics of taxon relative abundances is described by the Langevin equation:

$$\dot{x}_i = F_i \cdot x_i^{\alpha} + V \cdot x_i^{\beta} \xi_i(t) - \phi(t) \cdot x_i,$$ (1)

where F_i captures the fitness of the taxon i, V corresponds to the noise amplitude and $\xi_i(t)$ is a Gaussian random noise with zero mean $<\xi_i(t)> = 0$ and variance uncorrelated in time, $<\xi_i(t)\xi_i(t')> = \delta(t'-t)$, . The function $\phi(t)$ ensures the normalization at all times, $\sum x_i(t) = 1$, and corresponds to $\phi(t) = \sum F_i x_i^{\alpha} + \sum V x_i^{\beta} \xi_i(t)$. The temporal evolution of the probability that a taxon i has a relative abundance $x_i(t)$, P(x_i,t), is determined by the Fokker-Planck equation:

$$\frac{\partial P}{\partial t} = -\frac{\partial}{\partial x_i}[(F_i \cdot x_i^{\alpha} - \phi(t) \cdot x_i) \cdot P] + \frac{1}{2}\frac{\partial^2}{\partial x_i^2}(V^2 \cdot x_i^{2\beta} \cdot P).$$ (2)

The microbiota evolves towards a steady-state with a time-independent probability depending on the values of α, β, F_i and V. For $\alpha < 1$ (otherwise, systems are always unstable), the steady-state probability may be localized in a region around a preferred value or broadly distributed over a wide range, depending on whether the fitness F_i dominates or is overwhelmed by the noise amplitude V. The steady-state solution of the Fokker-Planck equation is given by:

$$P_0(x_i) = C_{ne}(\alpha, \beta, F_i, V) \cdot x_i^{-2\beta} \cdot \exp\left[\frac{2F_i}{V^2}\frac{x_i^{1+\alpha-2\beta}}{1+\alpha-2\beta} - \frac{\phi_0}{V^2}\frac{x_i^{2-2\beta}}{1-\beta}\right] \quad \text{if} \quad 2\beta \neq 1+\alpha,$$

$$P_0(x_i) = C_e(\alpha, \beta, F_i, V) \cdot x_i^{\frac{2F_i}{V^2}-2\beta} \cdot \exp\left[\frac{\phi_0}{V^2}\frac{x_i^{2-2\beta}}{1-\beta}\right] \quad \text{if} \quad 2\beta = 1+\alpha,$$

285 where $\phi_0 = (\sum_i F_i^{1/(1-\alpha)})^{1-\alpha}$ and C_{ne} and C_e are integrals that should be solved numerically

286 for the parameters of interest. The ordered phase happens when the solution has a maximum

287 in the physical interval $(0 < x_i < 1)$. For larger V, the transition to a disordered phase happens

288 when the maximum shifts to the unphysical region $x_i < 0$, which sets the phase transition

289 region $V(\alpha, \beta, F_i)$. The phase transition region can be calculated analytically in particular

290 cases:

$$F_i^2 = 4\beta\phi_0 V^2 \quad \text{if} \quad \beta = \alpha \neq 1,$$

$$F_i = \beta V^2 \quad \text{if} \quad 2\beta = 1 + \alpha,$$

293 where the first case, simplifies to $F = 3V^2$ if $\beta = 0.75$ and the fitness of this taxon dominates

294 in ϕ_0. In many physical systems (Brownian motion is the classical example), the two terms

295 of the Langevin equation are related. The _fluctuation–dissipation theorem_ states a general

296 relationship between the response to an external disturbance and the internal fluctuations

297 of the system (_59_). The theorem can be used as the basic formula to derive the fitness from

298 the analysis of fluctuations of the microbiota, assuming that it is in equilibrium (the ordered

299 phase).

300 Explain better the fluctuation-dissipation theorem

Selection and Methods

302 The bacteria and archaea taxonomic assignations were obtained by analysing 16S rRNA se-

303 quences, which were clustered into operational taxonomic units (OTUs) sharing 97 % se-

304 quence identity using QIIME (_43_). WGS data (_40_) were analysed and assigned at strain level

305 by the Livermore Metagenomic Analysis Toolkit (LMAT) (_44_), according to their default qual-

306 ity threshold. Genus, with best balance between error assignment and number of taxa, was

307 chosen as our reference taxonomic level. We have verified that our conclusions are not sig-

308 nificantly affected by selecting family or species as the reference taxonomic level (see Figure

309 7).

310 Specify, in each study treated, the nature of the samples (conditions, timespan

311 between timepoints, subjects). Specify, and it is very important, what we

312 consider *healthy* in each study (for example: pre-antibiotics is healthy)

Sample selection

314 We have chosen studies about relevant pathologies containing metagenomic sequencing time

315 data series of bacterial populations from humans in different healthy and non-healthy states.

316 We have selected only those individuals who had three or more time points of data available

317 in databases. Metadata of each study is provided in Tables **??** to **??**. All used 16S rRNA gene

318 sequencing except for the study of the discordant kwashiorkor twins (*40*) (see Tables **??** and

319 **??**) where shotgun metagenomic sequencing (SMS) and 16S rRNA were used. In the latter

320 case we selected to work with SMS data to show that our method is valid regardless of the

321 source of taxonomic information. Each one of the datasets was treated as follows:

16rRNA sequences processing

323 Reads from the selected studies were first quality filtered using the FastX toolkit (*60*), allowing

324 only those reads which had more than 25 of quality along the 75% of the complete sequence.

325 16S rRNA reads were then clustered at 97% nucleotide sequence identity (97% ID) into

326 operational taxonomic units (OTUs) using QIIME package software (*43*) (version 1.8) We

327 followed open reference OTU picking workflow in all cases. The clustering method used was

328 uclust, and the OTUs were matched against Silva database (*61*) (version 111, July 2012)

329 and were assigned to taxonomy with an uclust-based consensus taxonomy assigner. The

330 parameters used in this step were: similarity 0.97, prefilter percent id 0.6, max accepts 20,

331   max rejects 500.

Metagenomic sequences processing

Metagenomic shotgun (and 16S too) sequences were analyzed with LMAT (Livermore Metage-nomics Analysis Toolkit) software package (*44*) (version 1.2.4, with Feb'15 release of data base *LMAT-Grand*). LMAT was run using a Bull shared-memory node belonging to the team's HPC (high performance computing) cluster. It is equipped with 32 cores (64 threads available using Intel Hyper-threading technology) as it has 2 Haswell-based Xeons, the E5-2698v3@2.3 GHz, sharing half a tebibyte (0.5 TiB, that is, 512 gibibytes) of DRAM memory. This node is also provided with a card PCIe SSD as NVRAM, the P420m HHHL, with 1.4 TB, and 750000 reading IOPS, 4 KB, achieving 3.3 GB/s, which Micron kindly issued free of charge, as a sample for testing purposes. The computing node was supplied with a RAID-0 (striping) scratch disk area. We used the "Grand" database (*45*), release Feb'15, provided by the LMAT team, where "Grand" refers to a huge database that contains k-mers from all viral, prokary-ote, fungal and protist genomes present in the NCBI database, plus Human reference genome (hg19), plus GenBank Human, plus the 1000 Human Genomes Project (HGP) (this represent about 31.75 billion k-mers occupying 457.62 GB) (*45*). Previously to any calculation, the full database was loaded in the NVRAM. With this configuration the observed LMAT sustained se-quence classification rate was 20 kpb/s/core. Finally, it is worth mentioning that a complete set of Python scripts have been developed as back-end and front-end of the LMAT pipeline in order to manage the added complexity of time series analysis.

Taxa level selection

We selected genus as taxonomic level for the subsequent steps of our work. In order to ensure that, between adjacent taxonomic levels, there were not crucial differences which could still
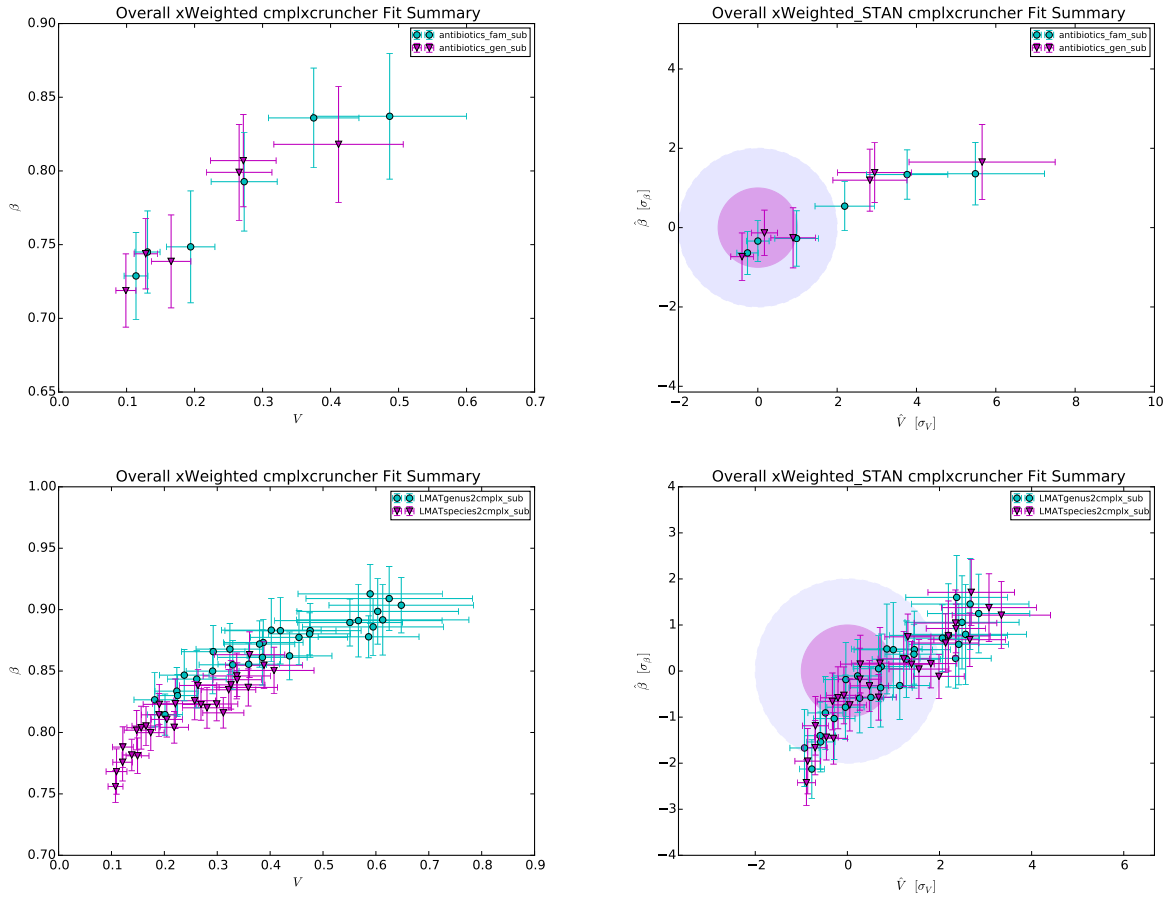
Figure 7. Overview of comparison of different approaches based on adjacent taxonomic levels using plots in the Taylor-parameters space. For 16S (former row of subfigures), the levels are family vs. genus, whereas for SMS (latter row of subfigures) levels are genus vs. species. The left column shows the raw results and the right column plots the standardized results (see Section)

be of relevance after standardization (see last subsection of Material and Methods), we tested two different data sets. In the former, the antibiotics study (*42*) with 16S data, we tested the differences between genus and family levels. The latter dataset tested was the kwashiorkor discordant twins study (*40*) for both genus and species taxonomic levels. The Figures 7 (overview) and 8 (detail) plot the comparison between studies (and so, 16S and SMS) and between adjacent taxonomic levels.
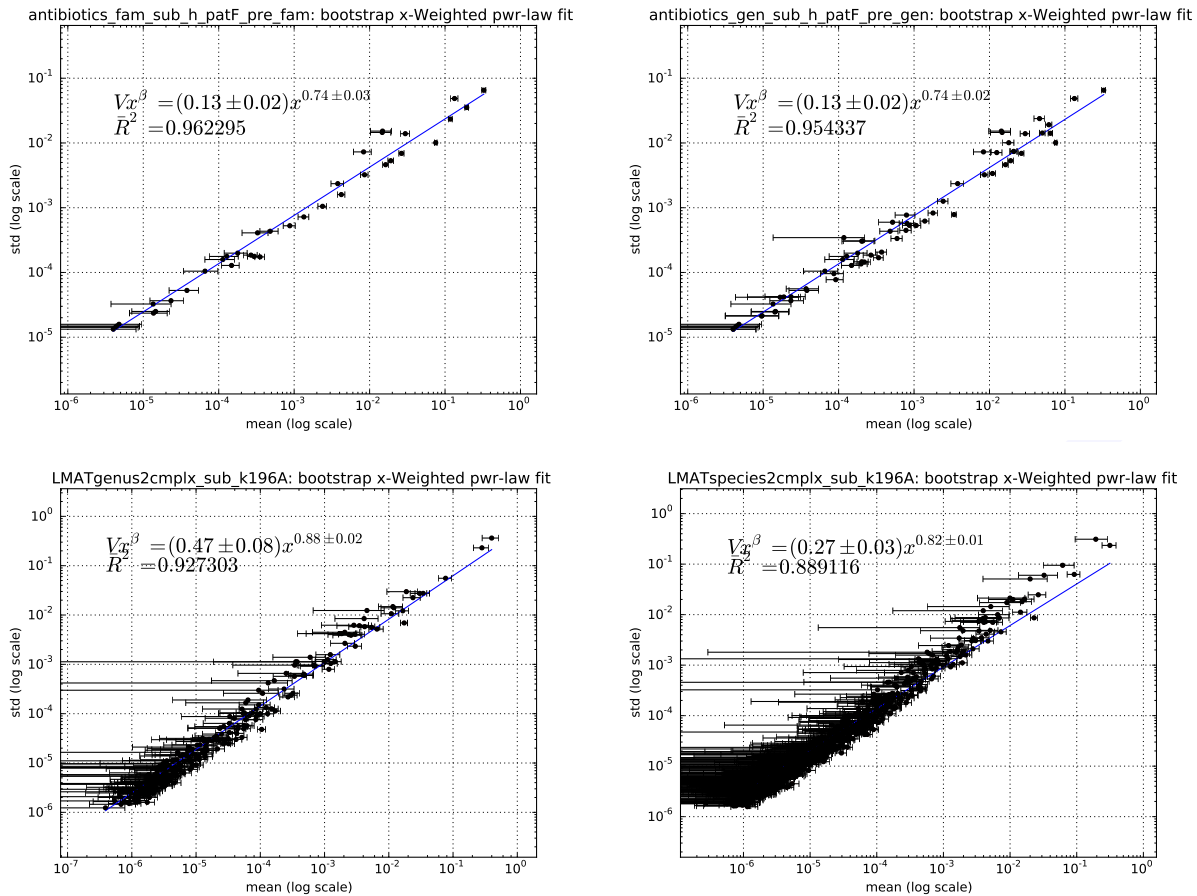
Figure 8. Detail of comparison of different approaches based on adjacent taxonomic levels using plots of X-weighted power-law fits (see Material and Methods). The former row of subfigures shows examples for 16S, whereas the latter row of subfigures plots examples for SMS. The left column shows results for the superior taxonomic level (family for 16S, genus for SMS), while the right column shows results for the inferior level (genus for 16S, specie for SMS).

X-weighted power-law fit

When fitting the power-law of std vs. mean, we can take into account that every mean has uncertainty and estimate it for a sample size *n* by the SEM (*Standard Error of the Mean*). Here, the uncertainties affect the independent variable, so the fit is not so trivial as a Y-weighted fit, where the uncertainties affect the dependent variable. A standard approach to do this fit is: a) invert your variables before applying the weights, b) then perform the weighted fit, and finally, c) revert the inversion. This method is deterministic, but the approximate solution worsens with smaller coefficients of determination. To overcome this limitation, we developed a stochastic method by using a bootstrapping-like strategy that avoids the inversion and is applicable regardless of the coefficient of determination.

The basic idea of bootstrapping is that inference about a population from sample data (sample → population) can be modeled by resampling the sample data and performing inference on (resample → sample). To adapt this general idea to our problem, we resample the x-data array using its errors array. That is, for each replicate, a new x-data array is computed based on:

$$x_i^* = x_i + v_i$$

where v_i is a Gaussian random variable with mean $\mu_i = 0$ and standard deviation $\sigma_i = \text{SEM}_i$, as defined previously. For each replicate a complete un-weighted power-law fit is performed, where to choose between fitting power laws ($y = Vx^\beta$) using linear regression on log-transformed (LLR) data versus non-linear regression (NLR) we mainly follow *General Guidelines for the Analysis of Biological Power Laws* (*62*). The parameters of the X-weighted fit are then estimated by averaging through all the replicate fits performed, and their errors are estimated by computing the standard deviation also for all the fits. At the end of each step, the relative error is calculated by comparing the fit parameters estimation in the last step with the previous one. Finally, both the coefficient of determination of the fit and the coefficient

25

Case	Condition	Colour	Description
1	$1 \geq \text{RSI} > 0.99$	blue	constant rank
2	$\text{RSI} > 0.90$	green	highly stable rank
3	$\text{RSI} > 0.75$	orange	moderately stable rank
4	$\text{RSI} > 0.25$	red	unstable rank
5	$0.25 \geq \text{RSI} \geq 0$	**black**	very unstable rank

Table 1. Colour code of the RSI percentage text shown in Figure 4, following the first condition satisfied.

385 of correlation between the fit parameters are estimated by averaging.

386 **Rank Stability Index**

387 The Rank Stability Index (RSI) is shown as a percentage in a separate bar on the right of the

388 rank matrix plot shown in Figure 4. The RSI is strictly 1 for an element whose range never

389 changes over time, and is strictly 0 for an element whose rank oscillates between the extremes

390 from time to time. So, RSI is calculated, per element, as 1 less the quotient of the number of

391 true rank hops taken between the number of maximum possible rank hops, all powered to p:

392
$$\text{RSI} = \left(1 - \frac{\text{true rank hops}}{\text{possible rank hops}}\right)^p = \left(1 - \frac{D}{(N-1)(t-1)}\right)^p$$

393 where D is the total of rank hops taken by the studied element, N is the number of elements

394 that have been ranked, and t is the number of time samples. The power index $p = 4$ is

395 arbitrarily chosen to increase the resolution in the stable region.

396 The colour code of the RSI percentage text in the rank plot shown in Figure 4 is chosen

397 following the first condition satisfied from those shown in Table 1.

Standardization

In order to properly show all the studies under common axes, we decided to standardize the Taylor parameters using the group of healthy individuals for each study. With this approach, all the studies can be visualized in a shared plot with units of Taylor-parameters standard-deviation on their axes.

For a Taylor parameter, e.g. V, the estimate of the mean $(\widehat{V})$ for the healthy subpopulation, composed of h individuals, is:

$$\widehat{V} = \frac{1}{W_1} \sum_{i=1}^{h} V_i \omega_i = \sum_{i=1}^{h} V_i \omega_i$$

as $W_1 = \sum_{i}^{h} \omega_i = 1$, since ω_i are normalized weights calculated as:

$$\omega_i = \frac{\frac{1}{\sigma_{V_i}^2}}{\sum_{i}^{h} \frac{1}{\sigma_{V_i}^2}}$$

being σ_{V_i} the estimation of the uncertainty in V_i obtained together with V_i from the X-weighted power-law fit described in Section , for healthy individuals.

Likewise, the estimation of the standard deviation for the healthy population $(\widehat{\sigma}_V)$ is:

$$\widehat{\sigma}_V = \sqrt{\frac{1}{W_1 - \frac{W_2}{W_1}} \sum_{i=1}^{h} \left[\omega_i \left(V_i - \hat{V} \right)^2 \right]}$$

being $W_2 = \sum_{i}^{h} \omega_i^2$, which finally yields to:

$$\widehat{\sigma}_V = \sqrt{\frac{1}{1 - \sum_{i}^{h} \omega_i^2} \sum_{i=1}^{h} \left[\omega_i \left(V_i - \hat{V} \right)^2 \right]}$$

Acknowledgments

Funding Information

References

1. **Rosenberg E, Zilber-Rosenberg I.** 2016. Microbes Drive Evolution of Animals and Plants: the Hologenome Concept. MBio **7**:e01395–15–.

2. **Bordenstein SR, Theis KR.** 2015. Host Biology in Light of the Microbiome: Ten Principles of Holobionts and Hologenomes. PLOS Biol **13**:e1002226.

3. **Swann JR, Want EJ, Geier FM, Spagou K, Wilson ID, Sidaway JE, Nicholson JK, Holmes E.** 2011. Systemic gut microbial modulation of bile acid metabolism in host tissue compartments. Proc Natl Acad Sci **108**:4523–4530.

4. **Spencer MD, Hamp TJ, Reid RW, Fischer LM, Zeisel SH, Fodor AA.** 2011. Association between composition of the human gastrointestinal microbiome and development of fatty liver with choline deficiency. Gastroenterology **140**:976–986.

5. **Samuel BS, Shaito A, Motoike T, Rey FE, Backhed F, Manchester JK, Hammer RE, Williams SC, Crowley J, Yanagisawa M, Gordon JI.** 2008. Effects of the gut microbiota on host adiposity are modulated by the short-chain fatty-acid binding G protein-coupled receptor, Gpr41. Proc Natl Acad Sci **105**:16767–16772.

6. **Smith PM, Howitt MR, Panikov N, Michaud M, Gallini CA, Bohlooly-Y M, Glickman JN, Garrett WS.** 2013. The Microbial Metabolites, Short-Chain Fatty Acids, Regulate Colonic Treg Cell Homeostasis. Science (80-) **341**:569–573.

7. **Kimura I, Ozawa K, Inoue D, Imamura T, Kimura K, Maeda T, Terasawa K, Kashihara D, Hirano K, Tani T, Takahashi T, Miyauchi S, Shioi G, Inoue H, Tsujimoto G.** 2013. The gut microbiota suppresses insulin-mediated fat accumulation via the short-chain fatty acid receptor GPR43. Nat Commun **4**:1829.

8. **Maslowski KM, Vieira AT, Ng A, Kranich J, Sierro F, Di Yu, Schilter HC, Rolph MS, Mackay F, Artis D, Xavier RJ, Teixeira MM, Mackay CR.** 2009. Regulation of in-

flammatory responses by gut microbiota and chemoattractant receptor GPR43. Nature **461**:1282–1286.

9. **Qin J, Li Y, Cai Z, Li S, Zhu J, Zhang F, Liang S, Zhang W, Guan Y, Shen D, Peng Y, Zhang D, Jie Z, Wu W, Qin Y, Xue W, Li J, Han L, Lu D, Wu P, Dai Y, Sun X, Li Z, Tang A, Zhong S, Li X, Chen W, Xu R, Wang M, Feng Q, Gong M, Yu J, Zhang Y, Zhang M, Hansen T, Sanchez G, Raes J, Falony G, Okuda S, Almeida M, LeChatelier E, Renault P, Pons N, Batto J-M, Zhang Z, Chen H, Yang R, Zheng W, Li S, Yang H, Wang J, Ehrlich SD, Nielsen R, Pedersen O, Kristiansen K, Wang J.** 2012. A metagenome-wide association study of gut microbiota in type 2 diabetes. Nature **490**:55–60.

10. **Brown JM, Hazen SL.** 2015. The Gut Microbial Endocrine Organ: Bacterially Derived Signals Driving Cardiometabolic Diseases. Annu Rev Med **66**:343–359.

11. **Durbán A, Abellán JJ, Jiménez-Hernández N, Artacho A, Garrigues V, Ortiz V, Ponce J, Latorre A, Moya A.** 2013. Instability of the faecal microbiota in diarrhoea-predominant irritable bowel syndrome. FEMS Microbiol Ecol **86**:581–589.

12. **Gevers D, Kugathasan S, Denson LA, Vázquez-Baeza Y, Van Treuren W, Ren B, Schwager E, Knights D, Song SJ, Yassour M, Morgan XC, Kostic AD, Luo C, González A, McDonald D, Haberman Y, Walters T, Baker S, Rosh J, Stephens M, Heyman M, Markowitz J, Baldassano R, Griffiths A, Sylvester F, Mack D, Kim S, Crandall W, Hyams J, Huttenhower C, Knight R, Xavier RJ.** 2014. The treatment-naive microbiome in new-onset Crohn's disease. Cell Host Microbe **15**:382–392.

13. **Ridaura VK, Faith JJ, Rey FE, Cheng J, Duncan AE, Kau L, Griffi NW, Lombard V, Henrissat B, Bain JR, Michael J, Ilkayeva O, Semenkovich CF, Funai K, Hayashi DK, Lyle J, Martini MC, Ursell LK, Clemente JC, Treuren W Van, William A, Knight R, Newgard CB, Heath AC, Gordon JI, Kau AL, Griffin NW, Muehlbauer MJ.** 2013. Gut Microbiota from Twins Discordant for Obesity Modulate Metabolism in Mice Gut

Microbiota from Twins Metabolism in Mice. Science **341**:1241214.

14. **Turnbaugh PJ, Hamady M, Yatsunenko T, Cantarel BL, Duncan A, Ley RE, Sogin ML, Jones WJ, Roe BA, Affourtit JP, Egholm M, Henrissat B, Heath AC, Knight R, Gordon JI.** 2009. LETTERS A core gut microbiome in obese and lean twins. Nature **457**:480–484.

15. **Subramanian S, Huq S, Yatsunenko T, Haque R, Mahfuz M, Alam MA, Benezra A, DeStefano J, Meier MF, Muegge BD, Barratt MJ, VanArendonk LG, Zhang Q, Province MA, Petri WA, Ahmed T, Gordon JI.** 2014. Persistent gut microbiota immaturity in malnourished Bangladeshi children. Nature **510**:417–21.

16. **Moya A, Ferrer M.** 2016. Functional Redundancy-Induced Stability of Gut Microbiota Subjected to Disturbance. Trends Microbiol **24**:402–413.

17. **Marchesi JR, Adams DH, Fava F, Hermes GD a, Hirschfield GM, Hold G, Quraishi MN, Kinross J, Smidt H, Tuohy KM, Thomas L V, Zoetendal EG, Hart A.** 2015. The gut microbiota and host health: a new clinical frontier. Gut 1–10.

18. **Falony G, Joossens M, Vieira-Silva S, Wang J, Darzi Y, Faust K, Kurilshikov A, Bonder MJ, Valles-Colomer M, Vandeputte D, Tito RY, Chaffron S, Rymenans L, Verspecht C, De Sutter L, Lima-Mendez G, Dhoe K, Jonckheere K, Homola D, Garcia R, Tigchelaar EF, Eeckhaudt L, Fu J, Henckaerts L, Zhernakova A, Wijmenga C, Raes J.** 2016. Population-level analysis of gut microbiome variation. Science (80-) **352**:560–564.

19. **Zhernakova A, Kurilshikov A, Bonder MJ, Tigchelaar EF, Schirmer M, Vatanen T, Mujagic Z, Vila AV, Falony G, Vieira-Silva S, Wang J, Imhann F, Brandsma E, Jankipersadsing SA, Joossens M, Cenit MC, Deelen P, Swertz MA, Weersma RK, Feskens EJM, Netea MG, Gevers D, Jonkers D, Franke L, Aulchenko YS, Huttenhower C, Raes J, Hofker MH, Xavier RJ, Wijmenga C, Fu J.** 2016. Population-based

metagenomics analysis reveals markers for gut microbiome composition and diversity. Science (80-) **352**:565–569.

20. **Wu H, Tremaroli V, Bäckhed F.** 2015. Linking Microbiota to Human Diseases: A Systems Biology Perspective. Trends Endocrinol Metab **26**:758–770.

21. **Noecker C, Eng A, Srinivasan S, Theriot CM, Young VB, Jansson JK, Fredricks DN, Borenstein E.** 2016. Metabolic Model-Based Integration of Microbiome Taxonomic and Metabolomic Profiles Elucidates Mechanistic Links between Ecological and Metabolic Variation. mSystems **1**:e00013–15.

22. **Greenblum S, Turnbaugh PJ, Borenstein E.** 2012. Metagenomic systems biology of the human gut microbiome reveals topological shifts associated with obesity and inflammatory bowel disease. Proc Natl Acad Sci **109**:594–599.

23. **Taylor, L.R.** 1961. Aggregation, Variance and the mean. Nature **189,** 732-35.

24. **de Menezes MA, Barabási A-L.** 2004. Fluctuations in network dynamics. Phys Rev Lett **92**:1–4.

25. **Mantegna RN, Stanley HE.** 1995. Scaling behaviour in the dynamics of an economic index. Nature **376**:46–49.

26. **Eisler Z, Kertesz J, Yook SH, Barabasi AL.** 2005. Multiscaling and non-universality in fluctuations of driven complex systems. Europhys Lett **69**:664–670.

27. **Reed DH, Hobbs GR.** 2004. The relationship between population size and temporal variability in population size. Anim Conserv **7**:1–8.

28. **Anderson RM, Gordon DM, Crawley MJ, Hassell MP.** 1982. Variability in the abundance of animal and plant species. Nature **18**: 245–248

29. **Živković J, Tadić B, Wick N, Thurner S.** 2006. Statistical indicators of collective behavior and functional clusters in gene networks of yeast. Eur Phys J B **50**:255–258.

30. **Kendal WS.** 2003. An Exponential Dispersion Model for the Distribution of Human Single Nucleotide Polymorphisms. Mol Biol Evol **20**:579–590.

31. **Zhang Z, Geng J, Tang X, Fan H, Xu J, Wen X, Ma ZS, Shi P.** 2014. Spatial heterogeneity and co-occurrence patterns of human mucosal-associated intestinal microbiota. ISME J **8**:881–93.

32. **Kaltz O, Escobar-Paramo P, Hochberg M, Cohen** JE. 2012. Bacterial microcosms obey Taylor's law: Effects of abiotic and biotic stress and genetics on mean and variance of population density. Ecol Process **1**:5.

33. **Ramsayer J, Fellous S, Cohen JE, Hochberg ME.** 2012. Taylor's Law holds in experimental bacterial populations but competition does not influence the slope. Biol Lett **8**:316–319.

34. **Pérez-Cobas AE, Artacho A, Ott SJ, Moya A, Gosalbes MJ, Latorre A.** 2014. Structural and functional changes in the gut microbiota associated to Clostridium difficile infection. Front Microbiol **5**:1–15.

35. **Ding T, Schloss PD.** 2014. Dynamics and associations of microbial community types across the human body. Nature **509**:357–360.

36. **Gajer P, Brotman RM, Bai G, Sakamoto J, Schütte UME, Zhong X, Koenig SSK, Fu L, Ma ZS, Zhou X, Abdo Z, Forney LJ, Ravel J.** 2012. Temporal dynamics of the human vaginal microbiota. Sci Transl Med **4**:132ra52.

37. **Blumm N, Ghoshal G, Forró Z, Schich M, Bianconi G, Bouchaud J-P, Barabási A-L.** 2012. Dynamics of Ranking Processes in Complex Systems. Phys Rev Lett **109**:128701.

38. Caporaso, J.G. et al. Moving pictures of the human microbiome. *Genome Biol.* **12,** R50 (2011).

39. Faith, J.J. et al. The long-term stability of the human gut microbiota. *Science* **341,** 1237439 (2013).

40. Smith M.I. et al. Gut microbiomes of Malawian twin pairs discordant for kwashiorkor. *Science* **339,** 548-54 (2013).

41. David, L.A. et al. Diet rapidly and reproducibly alters the human gut microbiome. *Nature* **505,** 559-63 (2014).

42. Dethlefsen L., Relman D. A. Incomplete recovery and individualized responses of the human distal gut microbiota to repeated antibiotic perturbation. *Proc. Nat. Acad. Sci. USA* **108,** 4554-61 (2011).

43. Caporaso, J.G. et al. QIIME allows analysis of high-throughput community sequencing data. *Nature Methods* **7,** 335-6 (2010).

44. **Ames SK, Hysom DA, Gardner SN, Lloyd GS, Gokhale MB, Allen JE**. 2013. Scalable metagenomic taxonomy classification using a reference genome database. Bioinformatics **29**:2253-2260.

45. **Ames SK, Gardner SN, Marti JM, Slezak TR, Gokhale MB, Allen JE**. 2015. Using populations of human and microbial genomes for organism detection in metagenomes. Genome Res. **25**:1056-67.

46. Eisler,Z., Bartos,I., Kertesz,J. Fluctuation scaling in complex systems: Taylor's law and beyond. *Adv. Phys.* **57,** 85 (2008).

47. Jorgensen,B., Martinez,J.R., Tsao,M. Asymptotic behaviour of the variance function. *Scand. J. Statist..* **21,** 223-243 (1994).

48. Fronczak,A., Fronczak,P. Origins of Taylor's power law for fluctuation scaling in complex systems. *Phys. Rev. E* **81,** 066112 (2010).

49. Kendal, W.S., Jorgensen,B. Taylor's power law and fluctuation scaling explained by a central-limit-like convergence. *Phys. Rev. E* **83,** 066115 (2011).

50. Kendal, W.S., Jorgensen,B. Tweedie convergence: A mathematical basis for Taylor's power law. *Phys. Rev. E* **84,** 066120 (2011).

51. **Kilpatrick a M, Ives a R.** 2003. Species interactions can explain Taylor's power law for ecological time series. Nature **422**:65–68.

52. **Ballantyne IV F, J. Kerkhoff A.** 2007. The observed range for temporal mean-variance scaling exponents can be explained by reproductive correlation. Oikos **116**:174–180.

53. **Stein RR, Bucci V, Toussaint NC, Buffie CG, Rätsch G, Pamer EG, Sander C, Xavier JB.** 2013. Ecological modeling from time-series inference: insight into dynamics and stability of intestinal microbiota. PLoS Comput Biol **9**:e1003388.

54. **Fisher CK, Mehta P.** 2014. Identifying keystone species in the human gut microbiome from metagenomic timeseries using sparse linear regression. PLoS One **9**:e102451.

55. **Bucci V, Tzen B, Li N, Simmons M, Tanoue T, Bogart E, Deng L, Yeliseyev V, Delaney ML, Liu Q, Olle B, Stein RR, Honda K, Bry L, Gerber GK.** 2016. MDSINE: Microbial Dynamical Systems INference Engine for microbiome time-series analyses. Genome Biol **17**:121.

56. **Cohen JE, Xu M, Schuster WSF**. 2013. Stochastic multiplicative population growth predicts and interprets Taylor ' s power law of fluctuation scaling Stochastic multiplicative population growth predicts and interprets Taylor ' s power law of fluctuation scaling. Proc R Soc B Biol Sci **280**:20122955.

57. **Koenig JE, Spor A, Scalfone N, Fricker AD, Stombaugh J, Knight R, Angenent LT, Ley RE.** 2011. Succession of microbial consortia in the developing infant gut microbiome. Proc Natl Acad Sci **108** :4578–4585.

58. **Tikhonov M.** 2016. Community-level cohesion without cooperation. Elife **5**.

59. Weber, J. *et al.* Fluctuation dissipation theorem. *Phys. Rev.* **101**, 1620-6 (1956).

60. Gordon, A., Hannon, G.J. FASTX-Toolkit. FASTQ/A shortreads pre-processing tools (2010). http://hannonlab.cshl.edu/fastx_toolkit/ (accessed 23 Feb 2015).

61. Quast C. *et al.* The SILVA ribosomal RNA gene database project: improved data processing and web-based tools (2013)

62. Xiao Xiao, Ethan P. White, Mevin B. Hooten, and Susan L. Durham. On the use of log-transformation vs. nonlinear regression for analyzing biological power laws. *Ecology* **92**, 10, 1887-1894 (2011).

63. Magee L., R^2 measures based on wald and likelihood ratio joint significance tests. *The American Statistician* **44**, 3, 250-253 (1990).

64. Nagelkerke N.J.D., A note on a general definition of the coefficient of determination. *Biometrika* **78**, 3, 691-692 (1991).

65. Wu, C.F.J. Jackknife, bootstrap and other resampling methods in regression analysis. (with discussions) *The Annals of Statistics* **14**: 1261?1350 (1986)

Eliminar *et al.* y poner la referencia completa como exige la guía de estilo de la revista...